

Lesson 05 Surface Characterization

Preparation of surfaces

Most fundamental surface science studies are carried out with single crystals, particularly on the most compact surfaces, which are parallel to the lowest Miller index planes. This is because these are the most thermodynamically stable orientations and most widely found in crystalline materials. There are many procedures and techniques for cutting, orienting and polishing such samples.

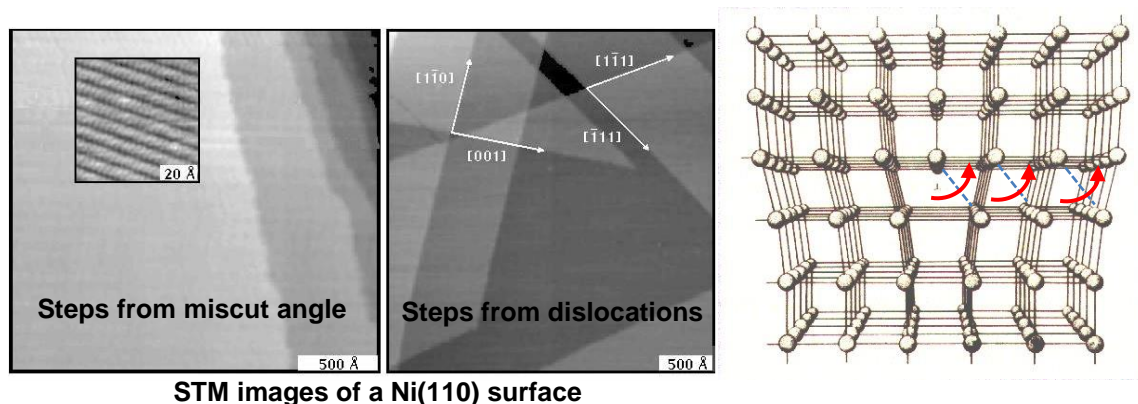
Orientation of the crystal is done with the help of Laue x-ray diffraction techniques (to be described later).

Cutting is done by use of diamond saws, and spark erosion techniques in the case of conductive samples. Ceramic materials, ionic crystals and semiconductors surfaces can also be prepared by cleavage inside or outside the vacuum chamber. Cleavage however produces only the lowest energy surfaces where cleavage takes place preferentially. On cut crystals a 0.5° miscut from the desired orientation is typical, and a 0.1° is considered very good for metals.

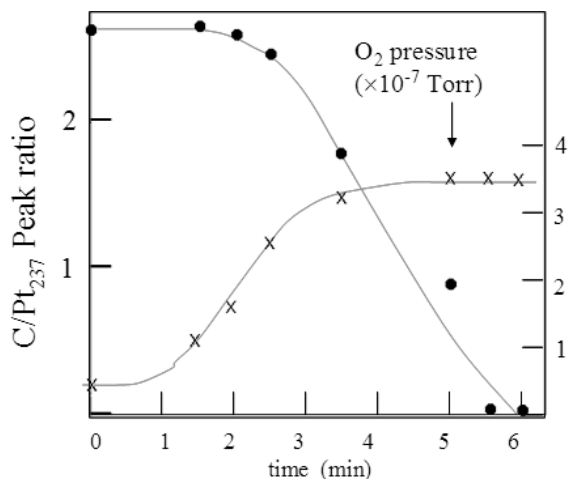
Polishing: Once cut, the surfaces are ground and polished using metallographic techniques based on the abrasive action of powders of hard materials, such as alumina, carbides, and diamond. The grain size of the polishing powder is decreased sequentially, until the finest grains, leaving a highly reflective, mirror-like surface. The nice optical flatness of the surface after such polishing however is deceptive and in reality the surface is made of a polycrystalline layer, at least as thick as the size of the polishing grain used. Sometimes, electrochemical polishing can be performed as well. Laue X-ray diffraction is used to ascertain the orientation of the surface after polishing. Because of the inherent limitations in the precision of the cutting tools, polishing and mechanical mounting, it is difficult to produce surfaces that are closer than a fraction of a degree.

Once inside the UHV chamber the task of preparing the surface continues. Heating to elevated temperatures helps recrystallize the surface layers by propagating the crystalline bulk order all the way to the top surface atoms. A side effect of heating is that it relieves internal stresses built-up during mechanical manipulation, such as clamping, cutting,

bending, etc. This produces dislocation nuclei in the bulk that zip across the material when heating provides the energy for the atoms to overcome diffusion barriers. Dislocations appear on the surface and can be recognized by straight steps crossing each other at crystallographic angles, such as 120° and 90° , that reflect the directions of easy dislocation faults, as shown in the example of the figure below.



Another side effect of heating is the alteration of the composition of the surface. Adsorbed contaminant material can be either decomposed leaving residues, desorbed or dissolved into the bulk of the crystal. In addition, heating often leads to segregation of impurities present in the bulk. For example, if all the dissolved contaminants present in a depth of 1 micrometer of a sample of 99.99% purity were to segregate to the surface, a monolayer thick film would be formed.



Removal of C from Pt(110) by reaction with O as measured by the ratio of Auger peak heights of C and Pt. Sample temperature 550°C.

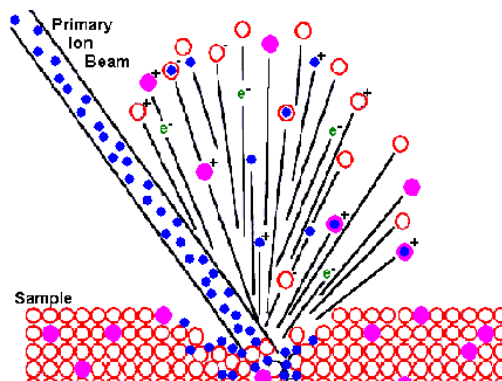
Removal of contaminant species is accomplished by physical or chemical methods.

Chemical methods are also used, which involve the use of reactive species for the removal of surface contaminants. For example, carbon can be “burned off” by heating the sample in a partial pressure of O₂. The sample is heated to a temperature in the range 500 to 800°C and O₂ gas is leaked in by means of

appropriate leak valves, to establish a background pressure of 10^{-7} or 10^{-6} torr. The O_2 molecules adsorb and dissociate on the surface so that the O atoms can react with surface C atoms to produce CO or CO_2 , which desorbs to the gas phase. One example of this process is shown in the figure. This procedure works quite well with noble metals like Pt, Rh, Ir, and others. It works also with more reactive metals, although in that case there is the side effect that excess O can be left on the surface in the form of an oxide, which needs to be removed by heating or by another chemical reaction with H_2 or CO.

Sputtering (Ion bombardement)

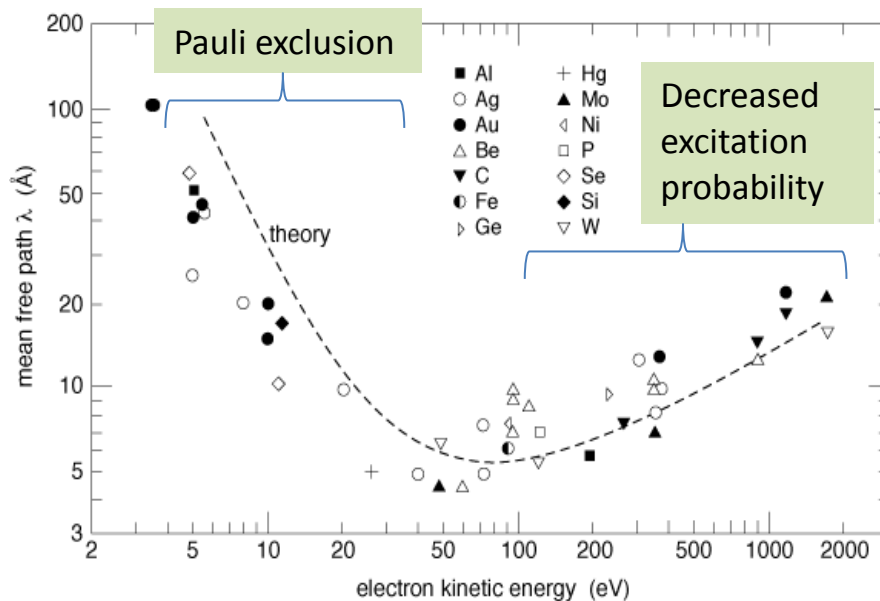
Physical methods involve the bombardment of the surface by an energetic beam of ions, typically Ar at 1 KeV. The kinetic energy of the ions is transferred to the atoms near the surface and results in their ejection. This is called also sputtering. Typical yield rates for energies around 1 KeV are close to 1. Thus for a beam current of 1 μA , we have $\sim 10^{-6}/10^{-19} = 10^{13}$ ions per second. Over a 1 cm^2 of the sample that means about 1 monolayer per minute is removed. Of course, both contaminants and sample atoms are removed at the same time since the sputtering cross section depends only weakly on the element. In addition a substantial amount of disorder is created by the energetic impacts, and some amount of the inert gas (Ar) might be left buried a few layers under the surface. Removal of the implanted Ar might require extensive heating at high temperature due to the random diffusion of the Ar atoms in the sample matrix. This is shown in the example of the figure, illustrating the removal of Ar implanted on a Pt(111) crystal. After sputtering it is then necessary to heat again at high temperature again to recrystallize and produce a clean, well-ordered sample.



Electron mean free path inside materials

When electrons travel inside a solid they interact strongly with core and valence electrons from the host lattice as well as with the ions, losing energy and changing directions at each event. The processes include excitation of transitions from valence and

Universal electron mean free path



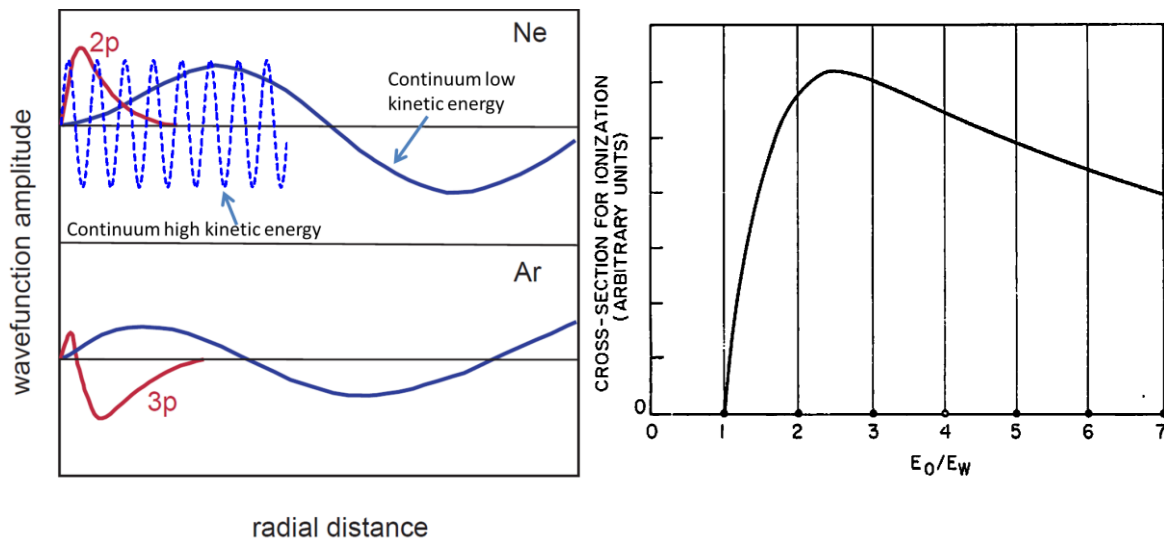
core states to unoccupied levels above the Fermi energy. The probability of exciting these transitions depends strongly on the electron energy. For example, to excite a core electron the incoming electron must have a kinetic energy equal or larger than the binding energy of the core level. The cross-section for core level ionization has been calculated by a number of approximate methods, by Bethe and by others.

Electrons with low energy can only lose energy by exciting valence band or molecular orbital electrons, in addition to phonons (meV) and plasmons (1-20 eV). Since both the excited electron and the primary electron have to occupy an empty level, which according to the Pauli exclusion principle can only accommodate two electrons of opposite spin, the number of available levels shrinks to zero as the primary electron energy decreases approaching the Fermi level. Therefore there is a strong reduction in inelastic cross-section when the electron energy is of only a few eV. The minimum λ occurs for electrons of energies around 100 eV where $\lambda \approx 0.5$ nm. Since λ depends on the electron energy E much more rapidly than on the chemical identity of the elements,

one speaks of a “universal” mean free path curve, partly justified by experimental results. Such a curve is shown in the figure above.

Cross section for ionization of a core level

Qualitatively, a lot can be learned about the ionization cross sections by looking at the radial part of the wave function of the electrons. The top graph in the figure shows the radial wave function $\phi_i(x,y,z)$ of an initial core level (Ne 2p, red color) together with the wave function of the electron after excitation $\phi_f(x,y,z)$ (solid blue color) by an incoming electron or photon of just enough energy to excite the core electron above the threshold, i.e. with enough kinetic energy (large wavelength) to escape the atom. Because the emitted electron is escaping free the wave function $\phi_f(x,y,z)$ is represented as a sinus



wave.

Qualitatively, the matrix element for this excitation is given by an integral that contains the product of the two wave functions: $\int \phi_f(x,y,z) |H| \phi_i(x,y,z) dx dy dz$, with H being the interaction operator (the electric field of the incident photon or the Coulomb potential of the incident electron). In order for this integral to be non-zero the two wave functions ϕ_i and ϕ_f must overlap in space in a non-destructive way.

When the incoming electron loses more energy the kinetic energy of the outgoing electron increases and its wavelength becomes smaller. As the wavelength increases from

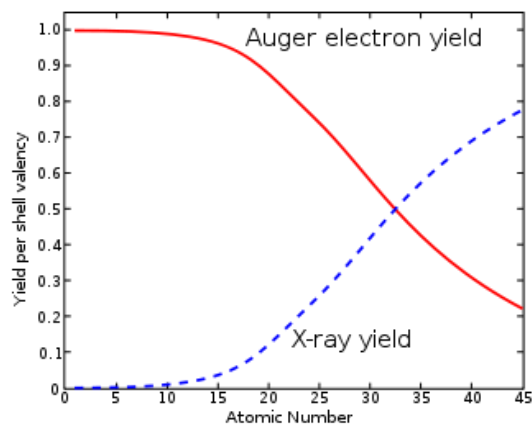
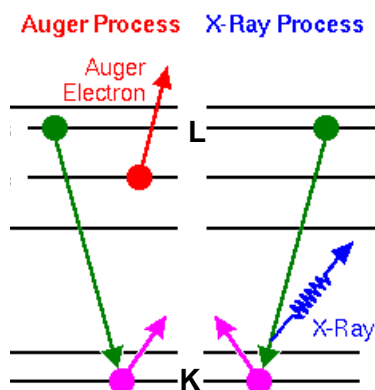
long to short value, at some point the spatial amplitudes of ϕ_i and ϕ_f match optimally and the value of the integral is maximum. At very high energies however, the wavelength of the outgoing electron will be so short (dashed blue line), that the integral contains very many positive and negative contributions of equal size and vanishes.

Therefore we expect the photoemission cross section to increase right after the threshold, rise to a maximum value, and then decrease slowly as the energy increases. The ionization cross-section reaches a maximum when the incident energy is between 2 and 3 times the binding energy of the core electron (figure on the right side).

Now consider the case of Ar 3p. The behavior here is qualitatively different because the radial wave function of the atom has a node. At the threshold the integral is negative but increases in absolute value. As the energy continues to increase a situation is reached where the first node of the outgoing wave divides the large negative area of the 3p area in almost equal parts. At this point, the integral will be close to zero. Upon a further increase of the energy, the integral will also increase again and finally, for very high energies, it will vanish for the same reasons as above. The minimum in the cross section for initial states where the wavefunction has a radial node is called a Cooper minimum.

Core level Spectroscopies

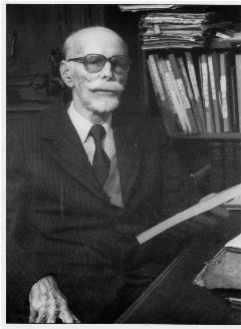
In these spectroscopies a core level, K for example, is ionized by an energetic particle, usually an electron or an x-ray. The core hole can decay by a transition of an



electron from an upper level, L for example, leading to the emission of a photon (called fluorescence decay), which obeys the dipole transition rules. The photon energy is:

$$h\nu = E_K - E_L$$

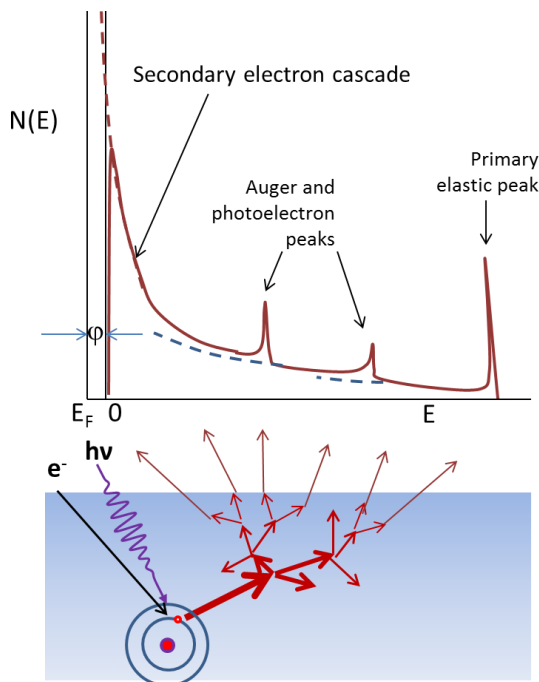
Another decay channel is the Auger process, which competes with the fluorescence channel. The Auger process involving XYZ levels (orbitals) arises from the electrostatic interactions in the ‘perturbed’ YZ levels due to the hole in X creates a non-symmetric charge distribution that repels the charge distribution in the other orbital (Z or Y). X-ray emission on the other hand is a dipole radiation transition due to the acceleration of the



Pierre Auger

electron from the upper level to the core hole. Emission is then favored in heavy elements where the initial core level has a large binding energy. For that reason Auger decay is predominant in low Z elements, or more precisely in transitions involving not too deep levels, while x-ray emission dominates for heavy elements or transitions involving deep core levels.

The strong interaction of electrons with matter, manifested in the very short mean free path, implies that during the escape to the surface the collisions generate numerous



secondary electrons of lower energy and in increasing numbers at ever lower energies due to the cascading effect. The result is an electron emission distribution $N(E)$ strongly peaked near zero kinetic energy. Auger and Photoelectron peaks are superimposed on this secondary electron cascade distribution, each one with its low energy tail of electrons that lost increasing amounts of energy. The figure illustrates the process and the distribution curve. The $N(E)$ curve reaches high values near the Fermi level, the work function barrier ϕ cuts off the slow electrons, as indicated.

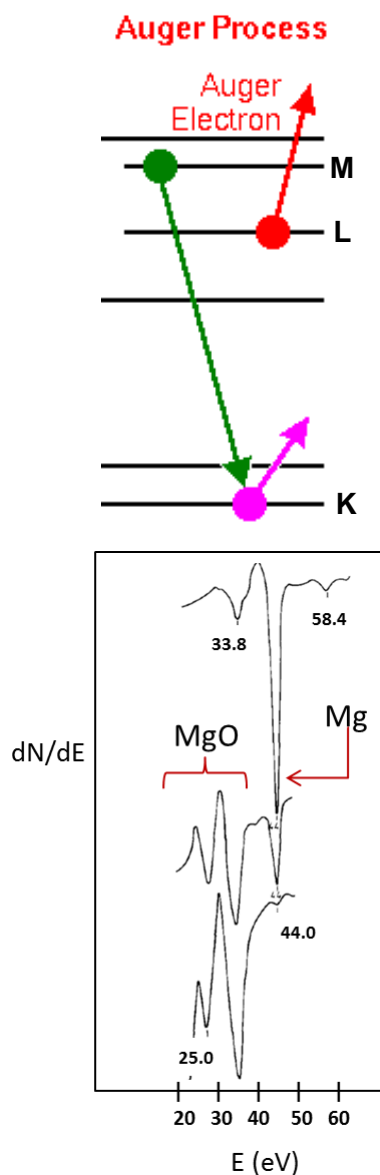
Auger Electron Spectroscopy

In this process, instead of a photon, another electron from a third level is emitted. If the binding energies of the three levels involved are E_K , E_L and E_M , the kinetic energy of the Auger electron is, in the first approximation: $E_{kin} = E_K - E_L - E_M$

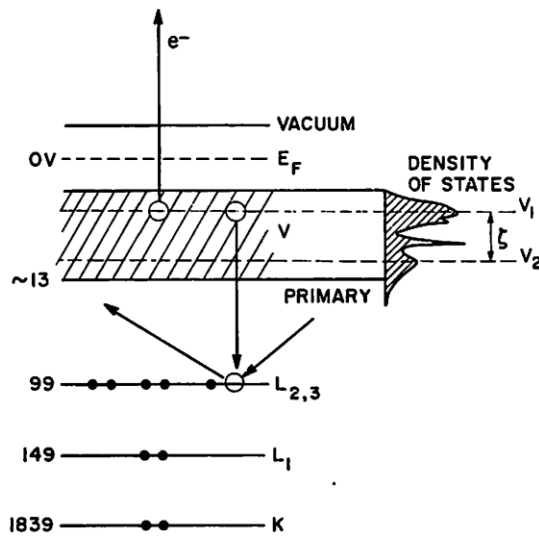
A better approximation is to use the energy of the same level in the next element of the periodic table because with a hole in the K level the other levels see a core with one more positive charge: $E_{kin} = E_K^Z - E_L^Z - E_M^{Z+1}$

Because the energies are characteristic of each element, the Auger peaks in an electron emission spectrum can reveal the identity of the elements on the sample. An Auger transition involving the X, Y, Z levels is labeled XYZ.

In addition to identify the parent element, the Auger transitions contain interesting information about its electronic structure. If for example the element is oxidized, i.e., it has lost electrons in the valence band, there is a shift (ΔE) in the energies of the core levels to higher binding energy. This is due to the fact that the tails of the wave function of the valence orbitals penetrate into the core region, so that removal of charge decreases the negative charge near the nucleus. If the shifts of the core levels were the same for all levels, the Auger energy of an oxidized atom would be: $E_{kin}^{oxid} = (E_K + \Delta E) - (E_L + \Delta E) - (E_M + \Delta E) = E_{kin} - \Delta E$, where E_{kin} is the energy of the same transition in the non-oxidized element. In reality the shifts are not the same and the formula does not give quantitatively correct values, but in a first approximation oxidation shifts the peak energies to lower values.



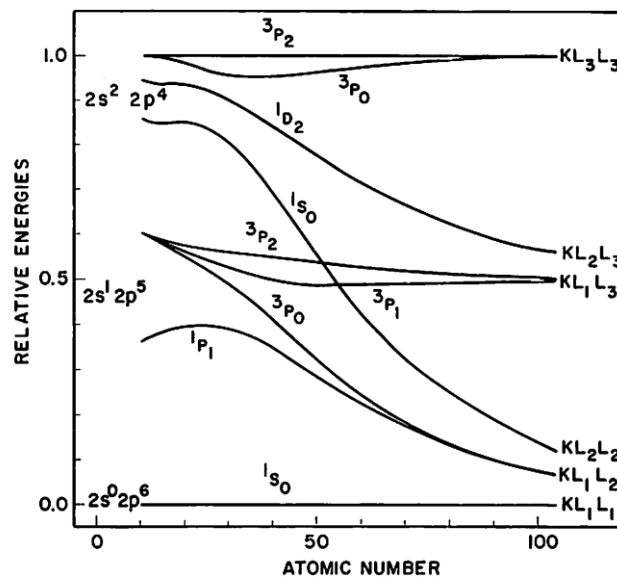
If one of the final state holes is in the valence band, the letter V is used to designate the transition, for example, KLV means an initial core hole in level K and the final holes in



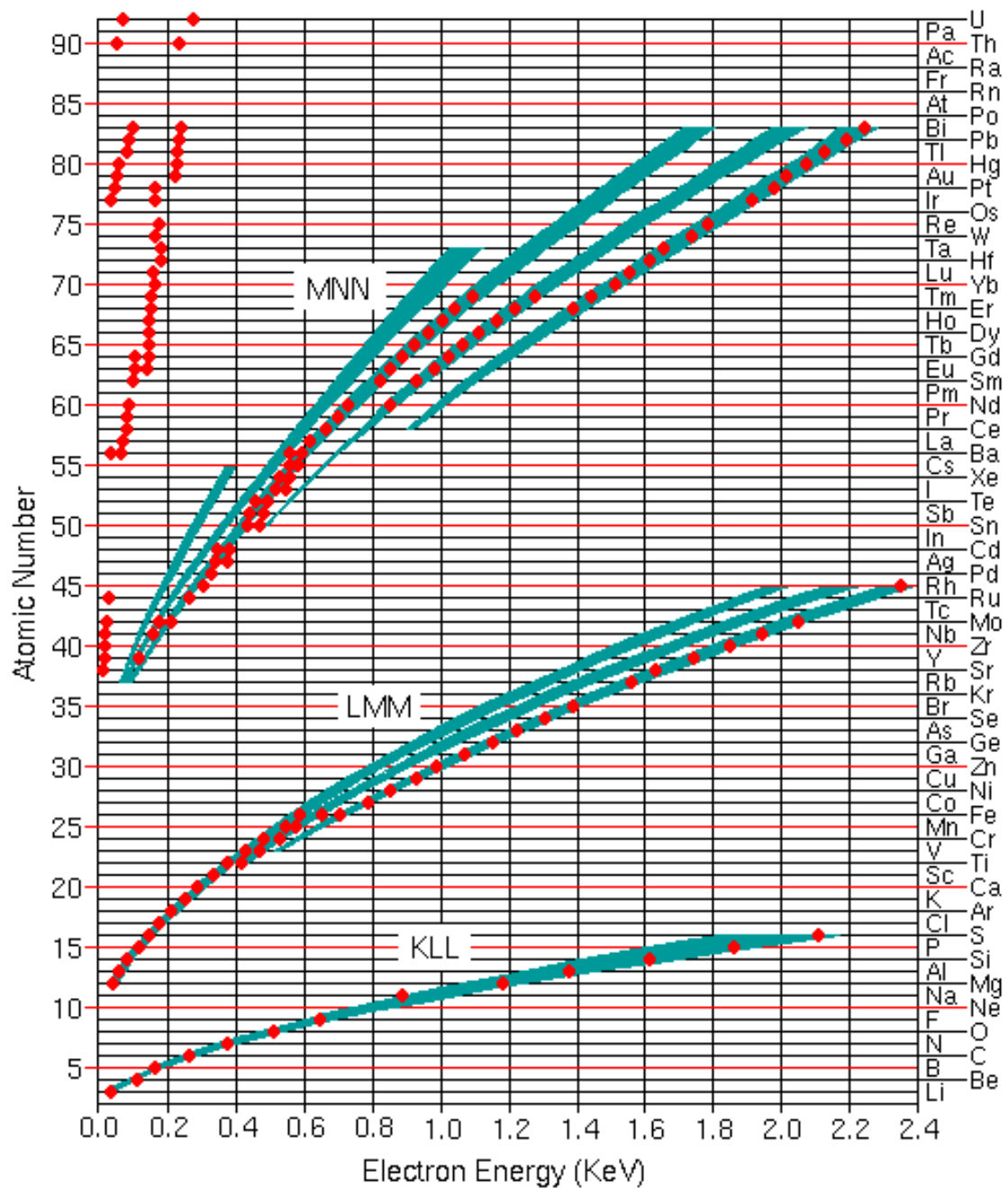
levels L (also a core level) and V (valence band level). If both holes are in the valence band the transition would be designated as KVV. The Auger peaks involving V levels have a width roughly equal to the width of the valence band for KLV, or twice that width for KVV (see figure).

Although the shape contains information on the density of states (DOS), directly for KLV, and self-convoluted for KVV, in practice it is difficult to extract the

DOS because of the strong perturbation from the hole-hole interactions. In fact the Auger peaks contain many satellite peaks each corresponding to a spectral term in the LS (light elements) or JJ (heavy elements) coupling between the spins and angular momenta of the two holes. The graph in the figure shows the energy spacing between the various spectroscopic terms (normalized to the 3P_2 and 1S_0 levels) when going from light elements (LS coupling) to heavy elements (JJ coupling).

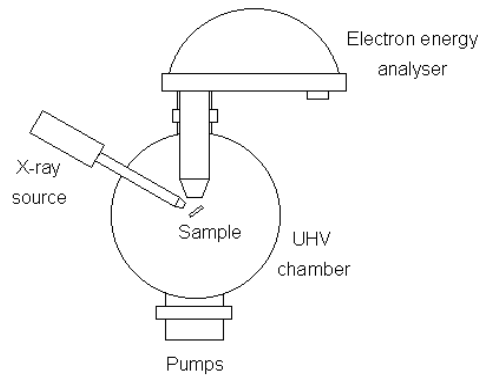


The graph below is a plot of all the important Auger peak energies of the elements across the periodic table.

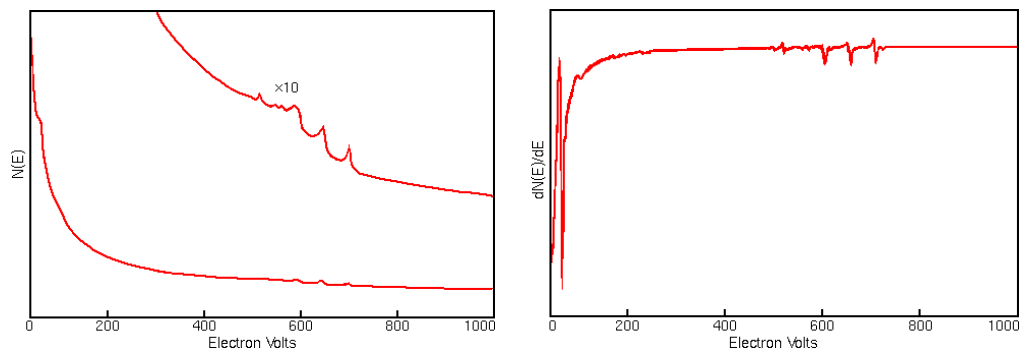


Experimental methods

Experimentally, to obtain AES spectra one uses either electrons or x-rays as primary excitation source. The most popular method is the first, because an electron gun is cheap and easier to operate than an x-ray source.



Because of the high secondary electron background from the losses on the incoming primary electron beam the Auger peaks need to be emphasized relative the large background. This is accomplished by differentiation of the emitted electron distribution curve $N(E)$. This can be done by modulating the electrode bias of the analyzed with a sinusoidal voltage and using a lock-in amplifier to extract the first harmonic, which is proportional to $dN(E)/dE$, while the second harmonic is proportional to $d^2N(E)/dE^2$. Example:

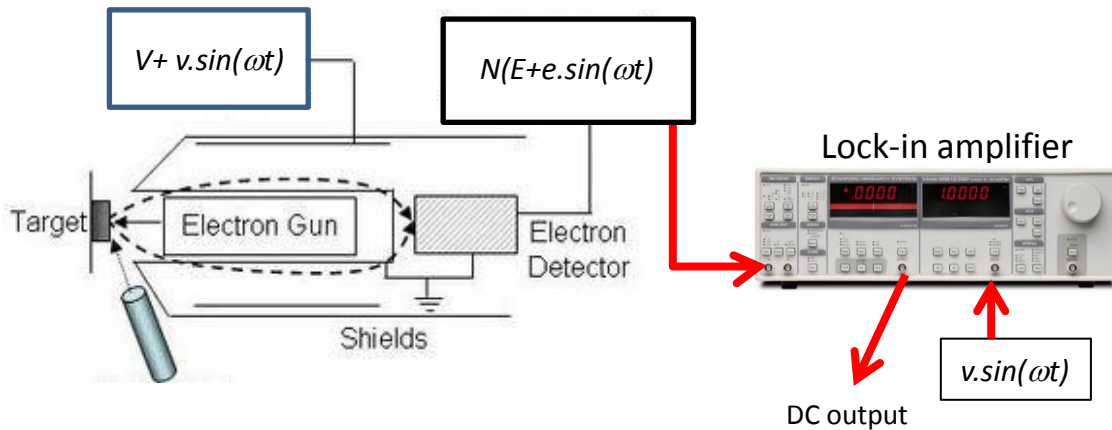


Method to obtain derivative spectra and to enhance signal/noise ratio

By adding a small periodic modulation signal $\sin(\omega t)$ to the scanning voltage one can obtain a significant increase in signal to noise ratio because the signal will now be an *ac* voltage that can be separated from the noise (which occurs at all frequencies) and filtered out. In addition the signal will have a fixed phase relative to the modulation, which allows for synchronous detection using Lock-in Amplifier.

Here is how it works. First expand the signal if a Fourier series:

$$N(E + e \cdot \sin(\omega t)) = N(E) + \frac{dN}{dE} \times e \cdot \sin(\omega t) + \frac{1}{2!} \frac{d^2N}{dE^2} \times e^2 \cdot \sin^2(\omega t) + \frac{1}{3!} \times \frac{d^3N}{dE^3} \times e^3 \cdot \sin^3(\omega t) + \dots$$



As can be seen the first harmonic, i.e., the *ac* term of frequency ω , has an amplitude, $e \cdot \frac{dN}{dE}$, proportional to the derivative.

The Lock-in amplifier first filters the incoming signal with a band-pass filter centered at frequency ω (or 2ω if so selected). This signal is then mixed with the reference modulation signal $v \cdot \sin(\omega_{ref} \cdot t)$ to generate output functions with frequencies $\omega - \omega_{ref}$ and $\omega + \omega_{ref}$. For our signal $\omega = \omega_{ref}$ so that there is an output that is *dc*. A low-pass filter at the output selects this signal which is proportional to the derivative spectrum.

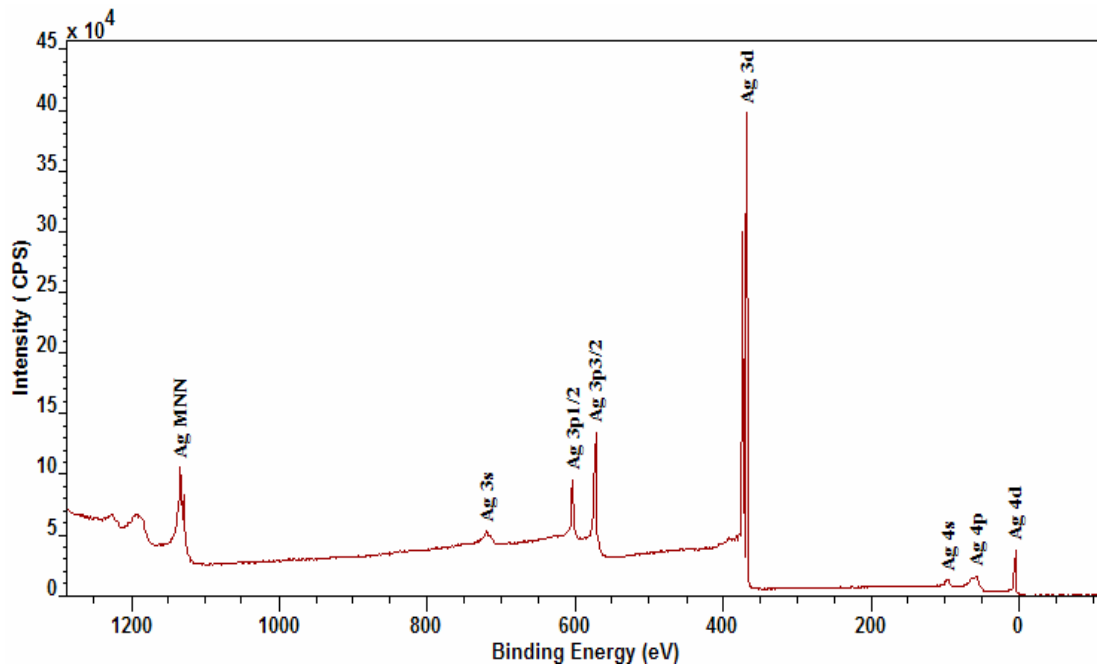
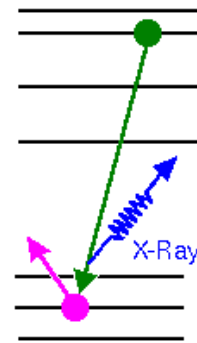
X-ray photoelectron spectroscopy (XPS)

In this spectroscopy one measures the energy of the electrons ejected from the core levels due to the absorption of an incident photon.

The figure below shows an example of a full XPS curve for Ag. These wide energy scans are called “survey spectra”. Although the energy axis from the spectrometer is the kinetic energy of the electrons, it is more common to convert the kinetic energy scale to a binding energy scale by subtracting the photon energy, as is done in the figure.

The energy distribution curve contains the photoelectron peaks from various Ag core levels as well as Auger peaks. Of course in spectra with the energy scale converted to binding energies, the Auger peaks appear at energies different from those in the tables. The increasing background as the kinetic energy decreases is clearly seen in the curve, with steps at the positions of major peaks.

X-Ray Process



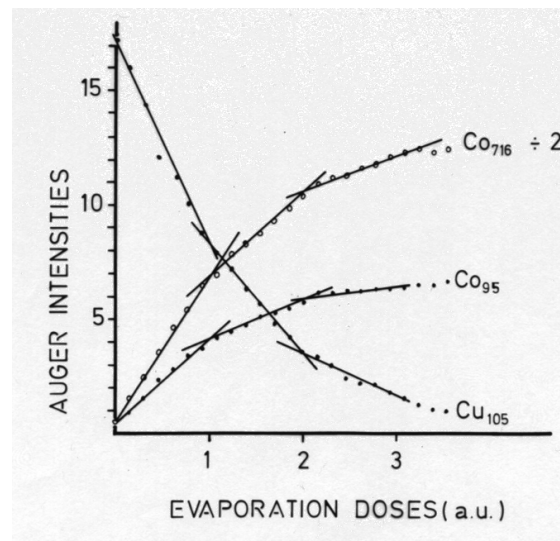
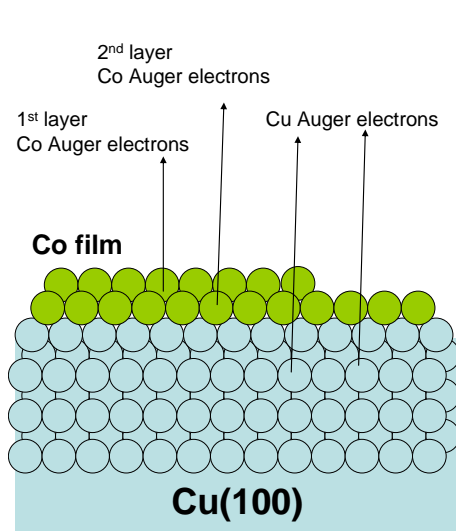
Widely used laboratory sources are made with Al and Mg anodes because they have intense lines from transitions to their ionized K levels with energies of 1253.6 eV (Al) and 1486.6 eV (Mg). Today we can use the much more powerful sources of the

Synchrotrons, which provide intense and broad band x-rays. We will come back to these sources later.

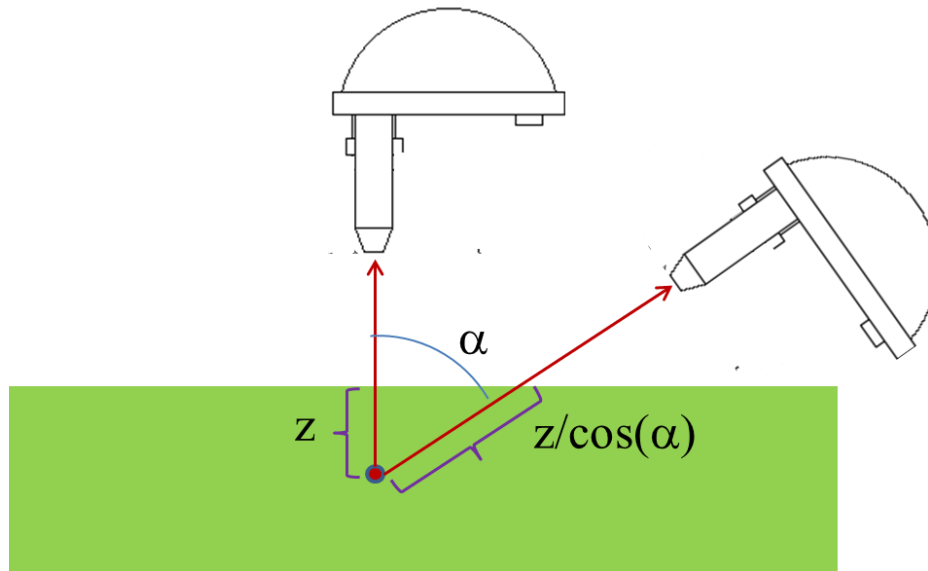
Use of the mean free path to study growth of materials and depth distribution

Knowing the mean free path we can calculate the decrease in intensity of an electron beam traveling in a material as a function of distance: The probability of an inelastic collision will increase exponentially with distance:

$$I(z) = I_0 \cdot \exp(-z/\lambda)$$

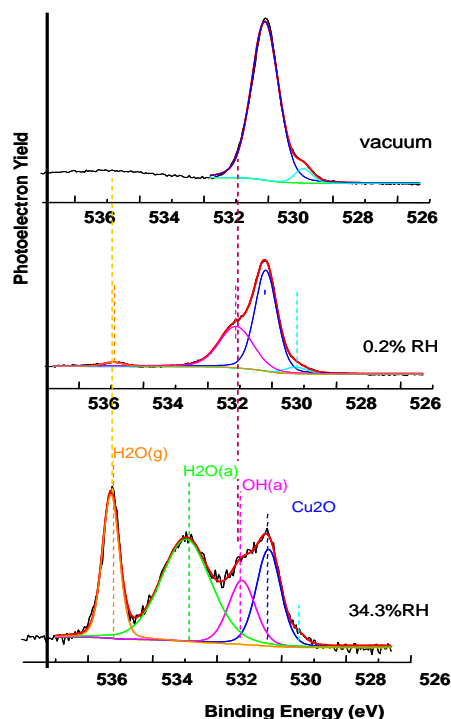


Another way to study depth distribution of a material is to record the intensity of its Auger peaks as a function of angle of emergence of the electrons, which can be done for example tilting the sample relative to the axis of the analyzer.



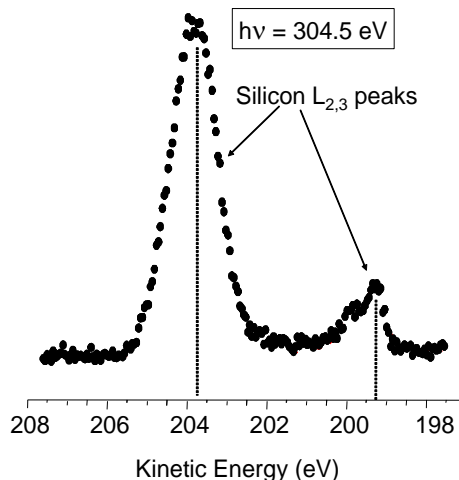
Chemical shifts

A very important characteristic of XPS is that the BE of the core levels is sensitive to the chemical state of the atom. This property was one of the major driving forces in popularizing the technique, particularly among chemists. In fact the XPS technique is also called ESCA, for Electron Spectroscopy for Chemical Analysis. The origin of this chemical sensitivity is very simple. As we explained above, if the atom loses valence electrons in a chemical bond (oxidized state) it costs a bit more energy to extract an electron from the core, because this electron feels less repulsion from the atom. These chemical shifts are also present in Auger spectroscopy but as we discussed the involvement of three levels complicates the interpretation relative to the straightforward XPS.

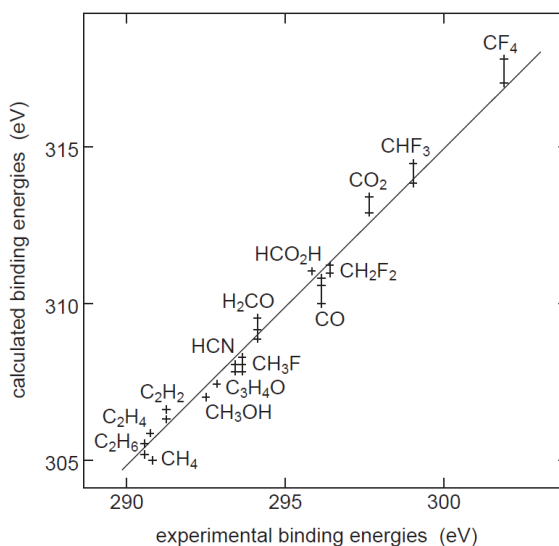


The examples in these figures illustrate the sensitivity of XPS to the chemical state of the atoms.

In the top left we have the O 1s region of a sample consisting of Cu₂O exposed to water. It shows



Carbon 1s BE in various molecules

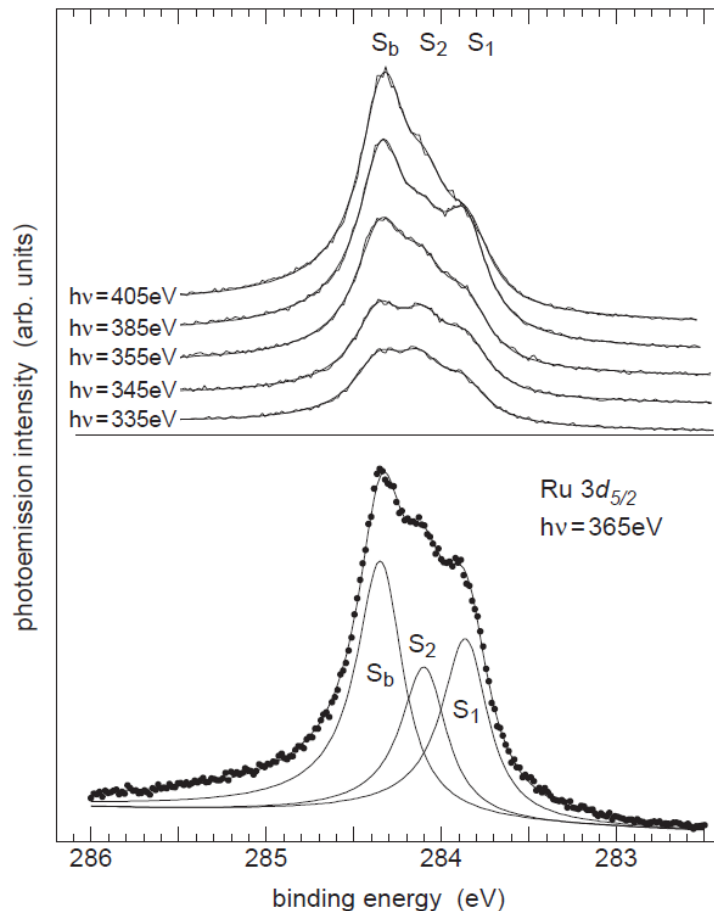


From: D.A. Shirley, Adv. Chem. Phys. 23, 85, (1973)

various chemical states of O: in the lattice bound to Cu, on the surface in the form of OH groups from dissociated water, and adsorbed molecular water. We can also see a gas phase peak from water.

Another example is the spectrum of the Si $L_{2,3}$ core levels, with clear differences between reduced and oxidized Si. Finally the graph shows the calculated and measured binding energies of C in a variety of compounds that clearly illustrates the power of XPS to determine both chemical identity and chemical state.

Surface and bulk core level shifts

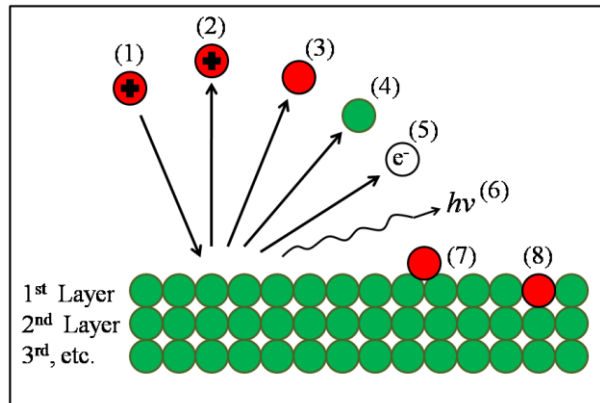


Ru $3d_{5/2}$ core level spectrum from the clean metal surface. Apart from the bulk peak two surface-related peaks are visible, one from the first and one from the second layer.

From: A. Baraldi et al., Phys. Rev. B. 61, 4534 (2000)

Surface Techniques involving ions

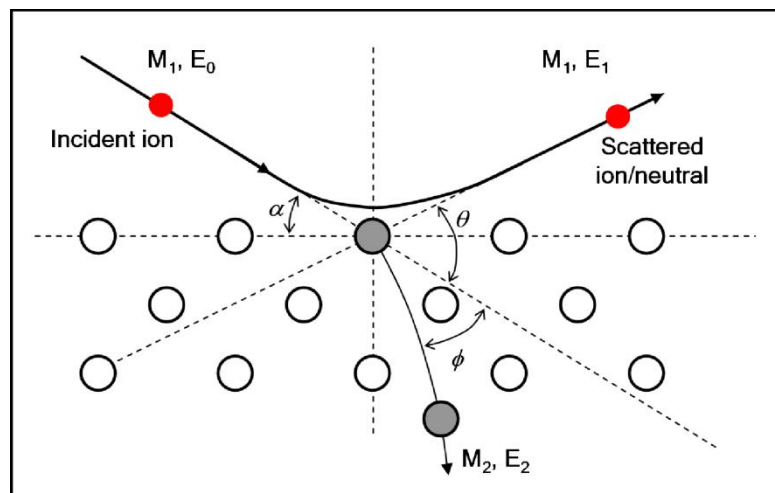
Several different types of events may take place as a result of the ion beam impinging on a target surface. Some of these events include electron or photon emission, electron transfer (both ion-surface and surface-ion), scattering, adsorption, and sputtering (i.e. ejection of atoms from the surface).



For each system and each interaction there exists an interaction cross-section, and the study of these cross-sections is a field in its own right.

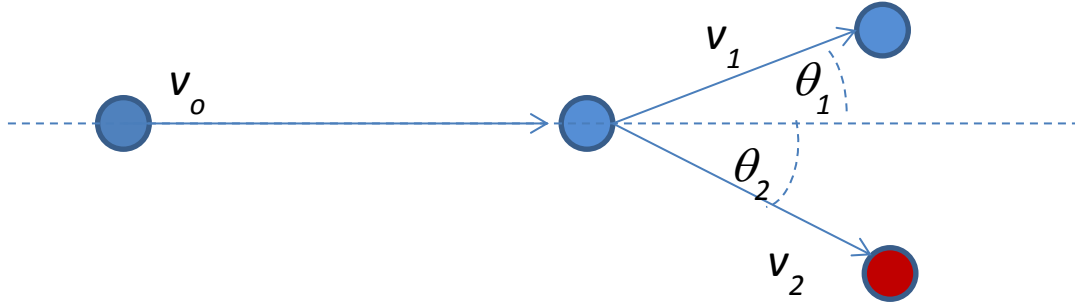
Ion Scattering Spectroscopies

In this technique we use the elastic collision with momentum transfer to identify the mass of the target atom. The figure illustrates the process: a beam of noble gas ions of typically 100 to 1000 eV is directed against the surface. The velocity of the scattered and recoil ions can be analyzed with spectrometers similar to those used for electrons.



Due to the energy range typically used in ion scattering experiments (> 500 eV), effects of thermal vibrations, phonon oscillations, and interatomic binding are ignored

since they are far below this range (~a few eV), and the interaction of particle and surface may be thought of as a classical two-body elastic collision problem. Measuring the energy of ions scattered in this type of interaction can be used to determine the elemental composition of a surface.



Two-body elastic collisions are governed by the laws of energy and momentum conservation. Consider a particle with mass m_0 , velocity v_0 , impacting another particle initially at rest with mass m . After scattering it is deflected by an angle θ and has a velocity v_1 , both of which can be measured. The target atom of unknown mass m recoils with velocity v_2 and angle $-\theta$.

We have:

$$E_0 = \frac{1}{2} m_0 v_0^2, \quad E_1 = \frac{1}{2} m_0 v_1^2, \quad E_2 = \frac{1}{2} m v_2^2 \quad (1)$$

Conservation of energy: $E_0 = E_1 + E_2$,

Conservation of momentum: $m_0 v_0 = m_0 v_1 \cos \theta_1 + m v_2 \cos \theta_2$

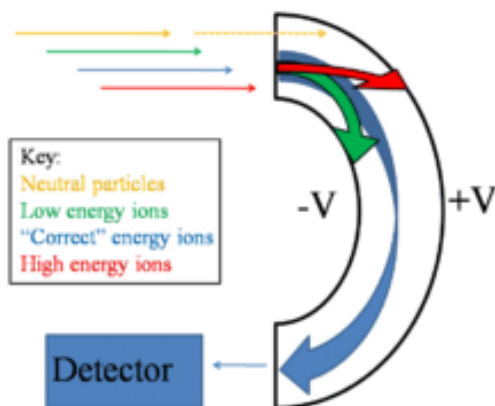
Solving for E_1 we get:

$$E_1 = E_0 \left(\frac{m_0 \cos \theta_1 \pm \sqrt{m^2 - m_0^2 \sin^2 \theta_1}}{m + m_0} \right)^2, \quad E_2 = E_0 \frac{4m \times m_0 \cos^2 \theta_1}{(m + m_0)^2} \quad (2)$$

It is clear that for $m < m_0$ the scattering angle $\theta < 90^\circ$. For the simple case of $\theta = 90^\circ$,

$$m = m_0 \frac{E_0 + E_1}{E_0 - E_1} \quad (3)$$

It is easy to show that $\frac{1}{2} m_0 v_2^2 = (E_0 - E_1)$ and $\sin \theta_2 = m_0 v_1 / m v_2$



In a well-controlled experiment the energy and mass of the primary ions (E_0 and m_0 , respectively) and the scattering or recoiling geometries are all known, so determination of surface elemental composition is given by the correlation between E_1 or E_2 and m . Higher energy scattering peaks correspond to heavier

atoms and lower energy peaks correspond to lighter atoms.

The following schematic summarizes the various ion-surface interaction processes as a function of ion energy:

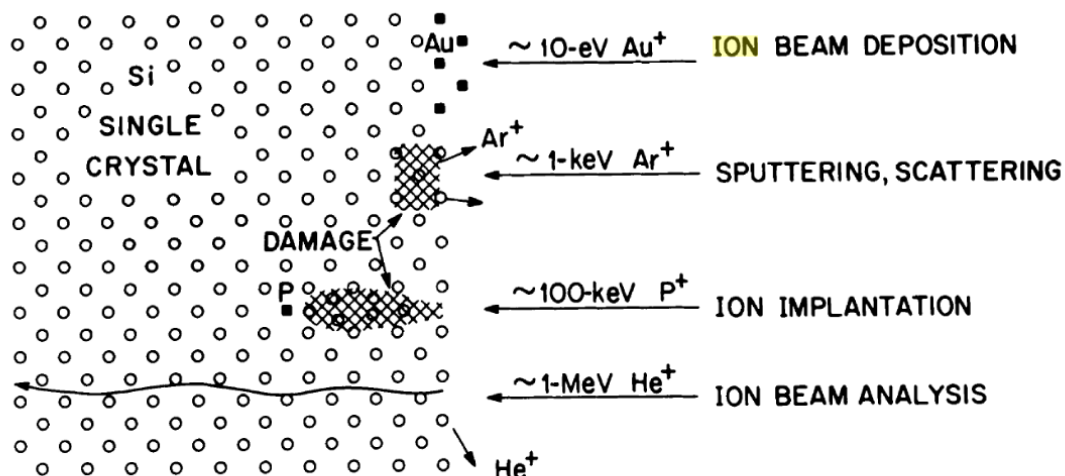


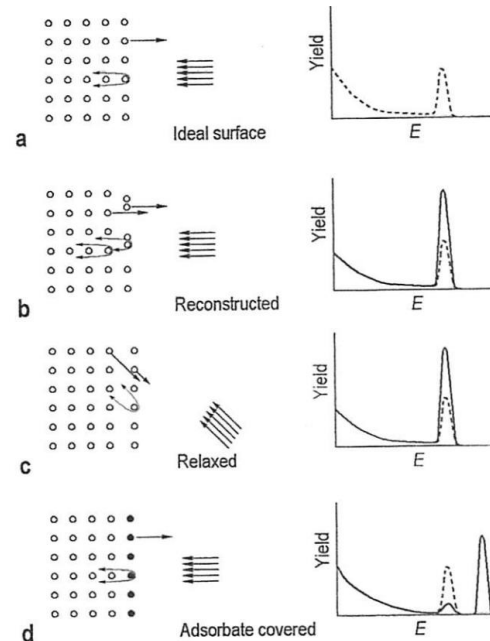
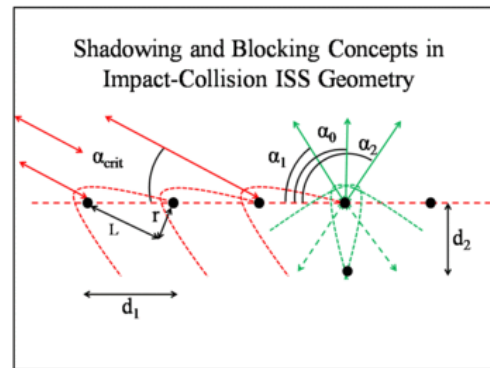
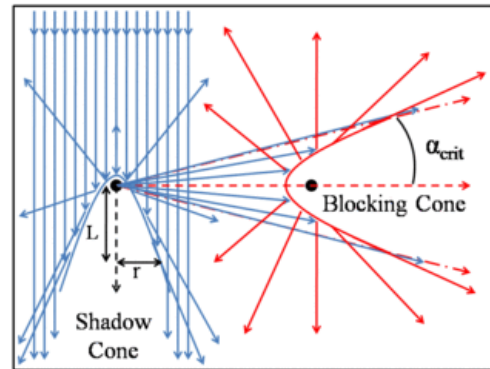
FIG. 1.1 Schematic illustrating the interactions of **ion** beams with a single-crystal solid. Directed beams of ~ 10 eV are used for film deposition and epitaxial formation. **Ion** beams of ~ 1 keV are employed in sputtering applications; ~ 100 -keV ions are used in **ion** implantation. Both of these processes damage and disorder the crystal. Higher energy light ions are used by **channeling** analysis.

From the book: *Materials Analysis by Ion Channeling*. C. Feldman, J.W. Mayer and S.T.A. Picraux. Academic Press Inc. 1982.

Shadowing and blocking:

Shadowing and blocking are important concepts in almost all types of ion-surface interactions and result from the repulsive nature of the ion-nucleus interaction. As shown at right, when a flux of ions flows in parallel towards a scattering center (nucleus), they are each scattered according by the Coulomb repulsion. This effect is known as shadowing. In a simple Coulomb repulsion model, the resulting region of “forbidden” space behind the scattering center takes the form of a paraboloid at a distance L from the scattering center. The flux density is increased near the edge of the paraboloid. The “size” of the shadowing cone depends strongly on the ion energy.

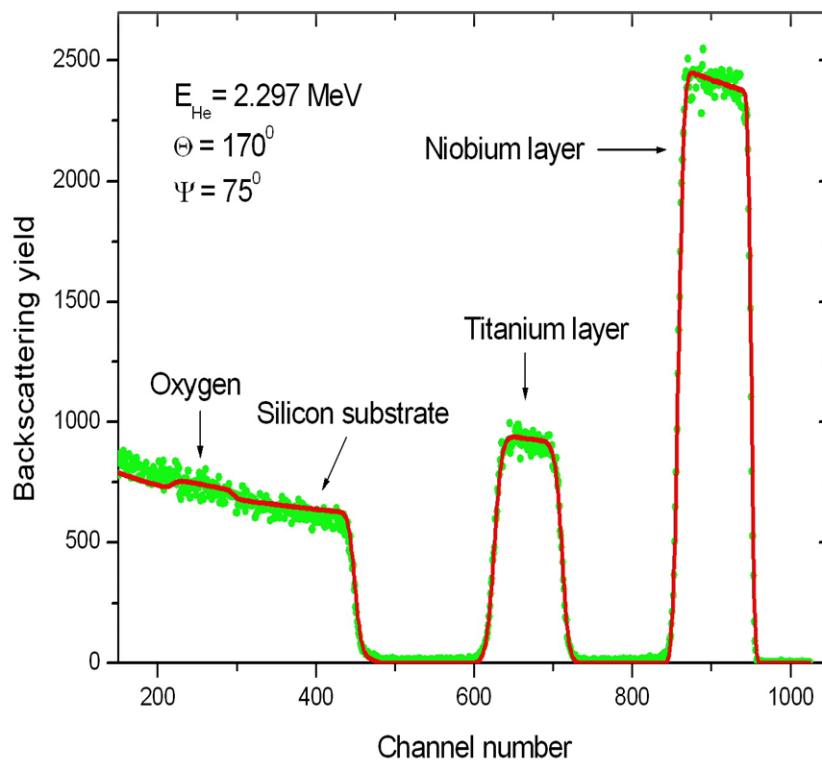
For example the cone radius of He^+ of 1 keV, $r \sim 1$ Å at a typical distance interatomic distance ($L \sim 3$ Å). At 100 keV, the cone radius is 0.2 Å, and at 1 MeV it is 0.09 Å. The shadow cone is associated with an increased ion flux at its edges (focusing effect). The shadowing effects can be used to advantage to study surface structure by measuring for example the yield of backscattered ions. The yield should be a minimum when the incident beam is aligned (see figures). By measuring the yield as a function of angle the position of atoms in the first few surface layers can be determined.



Rutherford Backscattering (RBS)

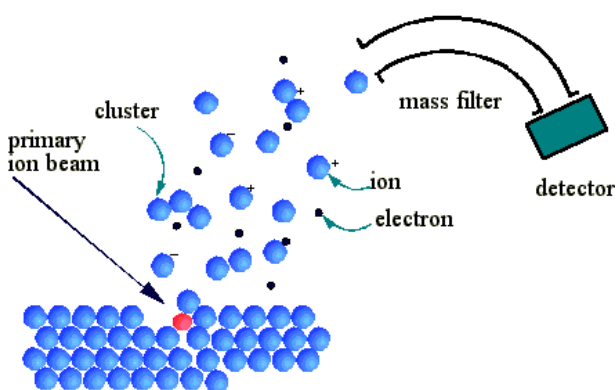
In this technique one measures the energy of the backscattered ions, which depends on their penetration depth inside the target material. The loss of energy is a function of the distance traveled inside and its rate dE/dz is called the stopping power, which is well known and tabulated for high energy ions (100 keV – 1 MeV).

The spectrum for a thin film of Nb on Ti on an oxidized Si wafer is shown in the figure. The high energy edge of the first peak and the lowest energy loss corresponds to ions scattered elastically from the top Nb layer, with energy given by formula (2) or (3). This is followed by a plateau (slightly increasing) of ions that have lost energy due to penetration, so that the width is proportional to the thickness and can be made quantitative using the known stopping power of Nb. This is followed by another peak due to a second layer of Ti, the high energy edge corresponding to the ions that lost energy corresponding to the mass of Ti (formula 2), plus the losses of penetration (in and out) through the Nb layer. Finally another edge marks the elastic collision (minus the losses from penetration the Nb and Ti layers) with the Si substrate.



Secondary Ion Mass Spectroscopy (SIMS)

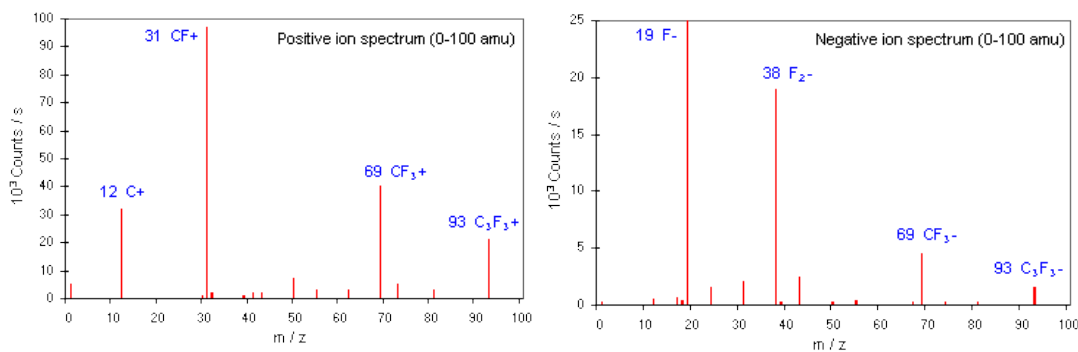
In SIMS an energetic ion beam impinges upon the sample to be analyzed and knocks off atoms, clusters of atoms and ions from the surface region. The ions (+ and -) are analyzed according to their mass to produce a spectrum of the surface composition.



The high signal-to-noise ratio of mass spectrometry makes the surface very sensitive, with detection limits as low as 10^{-8} monolayers ($\sim 10^7$ atoms per cm^2). This is the type of concentrations found in dopants of semiconductors and impurities that have an effect on the electronic properties of materials. The

yield however is highly sensitive to the “matrix”, i.e., to the chemical environment of the atom. For example the yield of Si^+ in pure Si is much lower, by factors of 1000's, to the yield in SiO_2 , because the electronegative O ions bound to the Si retain the electron when the Si atom is knocked –off by the primary ion.

The same is true for all other materials. Similarly the yield of negative ions depends strongly on the environment, oxidizing or reducing of the atom.



Because the collision can eject clusters of atoms, the SIMS spectrum provides information on the chemical surrounding of the atoms, for example an impurity atom surrounded by atomic species of the host material cannot give dimer, trimer and other clusters. Similarly the composition of the clusters contains information of the molecule that contains the atom.